

# Actuated Dynamic Walking in Biped Robots: Control Approach, Robot Design and Experimental Validation

David J. Braun *Member, IEEE*, Jason E. Mitchell and Michael Goldfarb, *Member, IEEE*

**Abstract**—This paper presents and experimentally demonstrates a control approach for actuated dynamic walking in biped robots. Rather than utilizing trajectory tracking, we proposed a control approach which employs state dependent control torques generated by low-gain spring-damper couples to encourage patterned motion of the robot. In order to verify that the control idea provides natural looking (human-like) dynamic walking, a seven-link biped robot was designed with backdrivable joint actuators, which allows passive leg motion. Following a discussion on robot design and the real-time control implementation, experimental data is presented to validate the proposed methodology.

**Index Terms**—Biped, dynamic walking.

## I. INTRODUCTION

IN recent years there has been considerable research effort devoted to bipedal locomotion. While various approaches are proposed in the literature, see Hurmuzlu *et al.* [1] for a review, most of the control methods either utilize the zero moment point (ZMP) paradigm, or rely on the (passive) dynamic walking principle.

The ZMP approach introduced by Vukobratović *et al.* [2], [3], [4] and applied or further developed by numerous authors [5], [6], [7], [8], [9], [10], is a well established method for biped locomotion synthesis. Application of this method has been shown to provide effective, robust, and versatile locomotion for biped robots, [11], [6]. As was pointed out in the literature however, utilization of trajectory tracking, relying on a characteristic bent knee stance support, and preferring a flat foot restriction, while walking, makes the ZMP-based walking control distinct from the one generally employed by humans, see [12], [13].

In order to achieve an efficient and natural-looking bipedal gait, several researchers have investigated a “dynamic walking principle” that emphasizes the significance of the passive (natural) dynamics of the robot through walking. On one end of this spectrum are fully passive dynamic walkers which rely on specific geometries and precisely tuned inertial robot design, and can walk on a slight downward slope powered only by gravity, [14], [15]. The same idea motivated development of actuator-assisted dynamic walkers (that utilizes a passive robot design) which have shown to possess human-like and energy efficient gait [16], [17], [18].

Actuated dynamic walking approaches which do not utilize the ZMP method (neither rely on a passive or a nearly passive robot design), have also been proposed in literature, see [19], [20]. In this context, a concept of “hybrid zero

dynamics” [21] and “virtual control constraints” [22] were used to develop and experimentally verify a walking control approach [23].

In order to synthesize natural looking compliant dynamic walking (without using considerable energy), backdrivable actuation has been recognized as important. In this light, Pratt *et al.* [24] have utilized “virtual model control” and “series-elastic actuators” to allow practical control realization which may not dictate, but (depending on the choice of control parameters) rather exploits the natural dynamics of the biped.

There are two main preconditions which allow natural-looking and energy-efficient realization of actuated dynamic walking. The first, related to the control approach, precludes enforcing a predefined reference trajectory and may also not favor enforcing state dependent kinematic constraints, or other attributes of the walking cycle (such as stride length, stepping frequency of average forward speed) with high gain control. This condition motivated us to develop a control framework which utilizes state-dependent control torques (generated by low-gain spring-damper couples) to provide motion coordination without prespecifying the response of the system. The second precondition (not related to control) depends on joint actuation which should not suppress passive joint motion (i.e., joints should be highly backdrivable such as human joints). Utilization of backdrivable joint design allows the inertial motion of the robot to be exploited through walking rather than being suppressed by the actuation units. Accordingly, to validate the control approach, a 7-link biped was designed with backdrivable joints which meets the second precondition (defined above) required for realization of actuated dynamic walking.

In the remainder of this paper, we describe our control approach, discuss the design of the seven link biped robot, comment on the real-time control implementation, and present data from walking experiments to demonstrate feasibility of the presented method.

## II. MODEL OF THE BIPED

In order to facilitate the controller development, we derive the dynamic model of the biped illustrated in Fig.1. The configuration of the biped is defined with nine coordinates,  $\mathbf{q} = [x, y, \theta, \theta_1, \theta_2, \theta_3, \theta_4, \theta_5, \theta_6]^T$ , where the first two coordinates characterize the translational motion of the robot in the inertial frame while the last seven angular coordinates reference the orientation of the links with respect to the inertial frame. The biped is considered actuated at each joint (i.e., right and left hip, knee, and ankle joints), such that, the dynamics of the robot are affected by six actuator torques,

The authors are with the Department of Mechanical Engineering, Vanderbilt University, Nashville, TN 37235 USA (david.braun@vanderbilt.edu; jason.mitchell@vanderbilt.edu; michael.goldfarb@vanderbilt.edu).

$\mathbf{u} = [u_1, u_2, u_3, u_4, u_5, u_6]^T$ , which are considered positive in the same (counterclockwise) direction as the joint angles. In order to support the forthcoming discussion, we will also define the joint angles (relative angles between the links) as:  $\varphi = [\varphi_1, \varphi_2, \varphi_3, \varphi_4, \varphi_5, \varphi_6]^T = [\theta_1 - \theta, \theta_2 - \theta_1, \theta_3 - \theta_2 + \pi/2, \theta_4 - \theta, \theta_5 - \theta_4, \theta_6 - \theta_5 + \pi/2]^T$ .

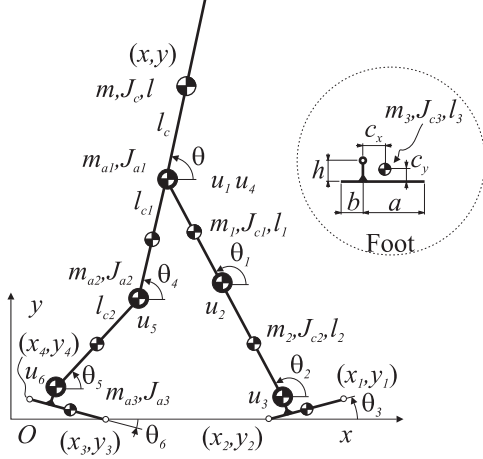


Fig. 1. Seven-link biped with the absolute coordinates  $\mathbf{q}$ , and the associated geometric and inertial parameters of the robot and the actuator units which generate the control torques  $\mathbf{u}$ . The Cartesian coordinates  $(x_i, y_i)$ ,  $i \in \{1, 2, 3, 4\}$ , represent the position of the toe and the heel for the left and right leg.

As follows, we derive the mathematical model by considering the biped as a constrained mechanical system, [25], [26], [27]. This model contains the differential equations of the flight phase motion, and the (algebraic and differential) relations which define the kinematic (physical) constraints along the motion. The model provides necessary information for the closed-loop control design.

1) *Unconstrained Dynamics*: The equations of motion for the 9-DoF (unconstrained) “flying” biped, can be written as

$$\mathbf{M}(\mathbf{q})\ddot{\mathbf{q}} + \mathbf{h}(\mathbf{q}, \dot{\mathbf{q}}) + \mathbf{G}(\mathbf{q}) = \mathbf{Q}_u, \quad (1)$$

where  $\mathbf{M} \in \mathbb{R}^{9 \times 9}$  is a symmetric and positive definite mass matrix,  $\mathbf{h} \in \mathbb{R}^9$  represents the normal and Coriolis inertial forces,  $\mathbf{G} \in \mathbb{R}^9$  represents the gravity terms, while  $\mathbf{Q}_u = \mathbf{E}\mathbf{u} \in \mathbb{R}^9$  is a generalized actuator force, calculated using a (constant) matrix  $\mathbf{E} \in \mathbb{R}^{9 \times 6}$  which defines the actuator arrangement on the robot.

2) *Kinematic Constraints*: For the biped in Fig.1, neither foot can penetrate the ground, the knee joints cannot extend beyond the fully straight position, and both feet are assumed not to slide when in contact with the ground. Since each toe and heel are independently characterized by non-penetration and no-slip with the ground, the flight phase dynamics (1) can be subject to the following kinematic (physical) constraints,

$$\Phi_h(\mathbf{q}) = \begin{bmatrix} y_1 \\ y_2 \\ y_3 \\ y_4 \\ \varphi_2 \\ \varphi_5 \end{bmatrix} = \mathbf{0}, \quad \Phi_n(\mathbf{q}, \dot{\mathbf{q}}) = \begin{bmatrix} \dot{x}_1 \\ \dot{x}_2 \\ \dot{x}_3 \\ \dot{x}_4 \end{bmatrix} = \mathbf{0}, \quad (2)$$

where  $(x_i, y_i)$ ,  $i \in \{1, 2, 3, 4\}$  are the toe and heel coordinates while  $\varphi_2$  and  $\varphi_5$  are the relative angles at the knee joint, see Fig.1. Instead of using (2) directly, the forthcoming control development only requires the information contained in the constraint matrix which is defined as,

$$\mathbf{A} = [(\partial\Phi_h/\partial\mathbf{q})^T, (\partial\Phi_n/\partial\dot{\mathbf{q}})^T]^T. \quad (3)$$

Depending on the configuration of the robot, the constraints in (2) and (3) are active when they restrict the motion, and inactive when they do not influence the dynamics. In order to ensure that  $\mathbf{A}$  only contains the active constraints, the configuration of the robot is monitored to identify and eliminate the inactive constraints by zeroing the corresponding row in (3). The constraint matrix obtained in this way carries the kinematic information from the configuration of the biped utilized in the forthcoming control development.

### III. CONTROL APPROACH

In this paper, the control methodology recently introduced for actuated dynamic walking in biped robots, [26], [27], is utilized. In the following, we briefly recall the main idea, and discuss the necessary ingredients for real-time implementation of the closed-loop walking controller.

The control approach considered here can be discussed in two stages. In the first stage, the robot is equipped with generalized control forces  $\mathbf{Q}_d$  which are (partially) referenced to the inertial frame to make generation of patterned movement intuitive. On a real robot however there is no associated control actuator which can realize the generalized control forces (referenced to the inertial frame) directly. Accordingly, in the second stage,  $\mathbf{Q}_d$  is recomputed to equivalent joint torques,  $\mathbf{u}$ , which are directly commanded through the robot joint actuators. As follows, we provide a systematic description of the outlined control idea on a seven link robot.

#### A. Generalized Control Forces

In order to generate patterned movement without any intent to utilize trajectory tracking, the seven link robot is provided with seven control elements which are spring-damper couples with fixed equilibrium points, see Fig.1. Each control element can be characterized with three control parameters, a stiffness constant, a damping constant, and an equilibrium angle. These parameters are changed as piecewise constant functions through four separate states along the walk using a configuration-based switching controller.

1) *Computing the Generalized Control Forces*: For a given set of control parameters, the desired generalized control force is computed as

$$\mathbf{Q}_d = -\mathbf{K}_d(\phi - \phi_d) - \mathbf{B}_d\dot{\phi}, \quad (4)$$

where  $\phi = [\theta, \theta_1, \varphi_2, \varphi_3, \theta_4, \varphi_5, \varphi_6]^T$  is obtained by position feedback,  $\dot{\phi}$  is known from a corresponding velocity feedback, while the control parameters concatenated in the stiffness matrix,  $\mathbf{K}_d$ , damping matrix  $\mathbf{B}_d$  and the equilibrium angles  $\phi_d = [\theta_d, \theta_{d1}, 0, \varphi_{d3}, \theta_{d4}, 0, \varphi_{d6}]^T$  are assigned by

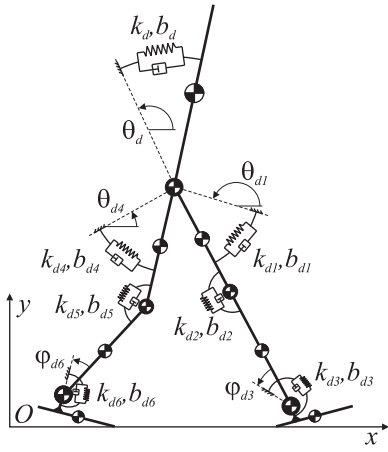


Fig. 2. The control elements and the control parameters on a 7-link robot.

the configuration-based switching controller as discussed in the forthcoming subsection.

While (4) has the same form as a usual PD control law, application of (4) in the present context is entirely different. Specifically, we utilize piecewise constant (fixed) equilibrium angles  $\phi_d$  along the motion of the robot instead of tracking a predefined desired trajectory  $\phi_d = \phi_d(t)$ . While this difference may not seem significant, one can recognize that it precludes high gains to be used by definition. Practically, high gains, with fixed angular references as depicted in Fig.2, would destabilize the robot instead of providing a good tracking performance usually required in trajectory tracking approaches.

2) *Parameter Modulation based on the Robot Configuration:* In order to achieve a walking motion, the control parameters are selected depending on the configuration of the robot. In this light, we define four separate states for each leg depending on whether the toe and/or the heel touches the ground and whether the leg is fully extended at the knee joint, see Fig.3.

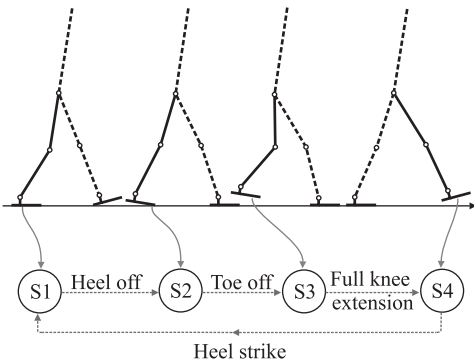


Fig. 3. The configuration-based switching logic with the four separate states. The particular state-flow,  $S1 \rightarrow S2 \rightarrow S3 \rightarrow S4 \rightarrow S1 \dots$ , together with the switching events, which correspond to normal walking, is indicated with dashed lines.

Utilizing the control elements which partially reference the inertial frame supports intuitive parameter tuning. As follows, we describe a biologically inspired approach for

the parameter selection with the intention to mimic muscle activation of walking human subjects, [28], [29].

While walking, one of the primary objectives is to keep the upper body in a upright vertical position. Utilizing the control element which acts between the body and the inertial reference frame one can set the stiffness parameter and the equilibrium angle to provide a near upright position for the upper body. A similar idea can be used to generate leg oscillation (with respect to a fixed inertial reference) by using the control elements attached to the thigh. Specifically, in swing, low stiffness and low damping elements pull the leg towards a fixed hip flexion configuration (specified with an equilibrium angle), while in stance, a higher stiffness and higher damping is assigned to the same control element, which encourages the stance leg to move towards a fixed hip extension angular configuration. The knee stiffness and damping are also modulated, by means of relatively high values in stance (to support the body with the help of the knee stop), and by employing only slight damping to generate nearly ballistic swing. The ankle is controlled by mimicking the strategy taken by humans. Accordingly, the ankle stiffness is used to accumulate elastic energy from the middle stance and provide a characteristic push-off at late stance. The main control parameter at the swinging ankle is an equilibrium angle which should be adjusted to provide slight dorsiflexion to avoid stumbling and/or scuffing.

### B. Actuator Torques

While  $\mathbf{Q}_d$  is straightforward to define, it does not represent the joint torques, and as such, it cannot be directly used to coordinate the motion of the robot. Practically, one may want to find the joint (motor) torques  $\mathbf{u}$  which, while directly commanded through the actuators, provide the same motion the robot would have by applying the desired generalized control forces  $\mathbf{Q}_d$ . In order to compute these torques, we propose a closed form analytical relation between  $\mathbf{Q}_d$  and  $\mathbf{u}$  as

$$\mathbf{u} = (\mathbf{N}\mathbf{R}^{-T}\mathbf{E})^+\mathbf{N}\mathbf{R}^{-T}\mathbf{Q}_d, \quad (5)$$

where  $\mathbf{R}$  is the upper triangular Cholesky factorization of the mass matrix,  $\mathbf{N} = \mathbf{I} - (\mathbf{A}\mathbf{R}^{-1})^+(\mathbf{A}\mathbf{R}^{-1})$  is the null-space projection operator of the inertially-weighted constraint matrix, while  $\mathbf{E}$  is a constant matrix which specifies the actuator arrangement on the robot. This control solution is derived with a primary objective to minimize the “acceleration energy”  $(\ddot{\mathbf{q}} - \ddot{\mathbf{q}}_d)^T \mathbf{M}(\ddot{\mathbf{q}} - \ddot{\mathbf{q}}_d)$  between the motion generated by the desired generalized control forces  $\ddot{\mathbf{q}}_d$  and the motion controlled by the actuator torques  $\ddot{\mathbf{q}}$ , and also to provide a minimum joint torque solution (minimize the squared Euclidean norm of the control torques) when the primary objective does not specify  $\mathbf{u}$  uniquely, see [26], [27]. Following the section on robot design, we will address the real-time control implementation where computation of (5) is further discussed.

## IV. ROBOT DESIGN

The 7-link biped robot, shown in Fig.4, is an experimental prototype which is 1.2m tall and weighs 14.3kg. The

geometric parameters and mass distribution on the robot are specified in Table.I. Below, we discuss the robot design, including a description of the modular joint design, foot design, the upper body and the sensory-system on the robot.



Fig. 4. Experimental prototype of a 7-link dynamic walker developed at the Vanderbilt University - Center for Intelligent Mechatronics

TABLE I

GEOMETRIC AND INERTIAL PARAMETERS OF THE ROBOT WITH TOTAL MASS OF  $M = 14.3kg$  AND HEIGHT OF  $L = 1.2m$ .

Structure	no. (*)	$l_*$ [m]	$l_{c*}$ [m]	$m_*$ [kg]	$J_{c*}$ [kgm <sup>2</sup> ]	
Body	—	0.390	0.185	6.12	0.021	
Thigh	1	0.295	0.147	0.67	0.0096	
Shank	2	0.298	0.14	0.55	0.0069	
Foot	3	0.183	—	0.36	0.0007	
Foot		$a$ [m]	$b$ [m]	$h$ [m]	$c_x$ [m]	$c_y$ [m]
		0.137	0.046	0.055	0.014	0.035
Actuators	no. (*)	$n_*$	$m_{a*}$ [kg]	$J_{a*}$ [kgm <sup>2</sup> ]		
Hip	1	21	0.84	0.0067		
Knee	2	12	0.84	0.0022		
Ankle	3	21	0.84	0.0067		

### A. Upper Body

The robot has a characteristic upper body which carries a 4.54kg, (10lb), mass located 0.2m from the hip joints, see Fig.4. The body is provided with a single-axis gyroscope (Analog Devices, ADXR150 with  $\pm 150^\circ/s$  measurement range) which directly measures the angular velocity of the body (in the sagittal plane). To reduce the noise level, the analog signal provided by the gyroscope is filtered with a first order (50Hz cutoff frequency) filter. The gyroscope is the only inertial sensor used in the proposed control implementation.

### B. Joint Design

The seven link robot has an upper body, hip, knee, ankle and human-like foot. In the current solution, a unified design

principle is utilized for the hip, knee and ankle joints with slight modifications made for differences in range of motion and attachment points. Fig.5 depicts the specific design solution of the knee joint. The robot is actuated with six 150W brushed DC-motors (Maxon RE40) through low gear ratio planetary reducers (Maxon GP42C), specifically 21 : 1, 12 : 1, 21 : 1 for the hips, knees and ankles respectively. A low gear ratio drive allows passive motion of the joints which is a precondition to leverage natural dynamics through actuated dynamic walking in biped robots. Each joint is provided with an incremental quadrature encoder (Maxon, ENC-MR-L-1024CPT) attached to the motor shaft. The reference position for each of the six encoders is identified (in a static stance phase during initialization) using two acceleration sensors located on the upper body and the upper right leg.

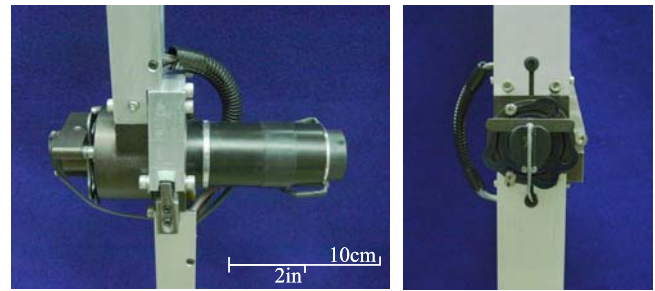


Fig. 5. Knee joint on the robot.

### C. Foot Design and the Foot Sensors

The foot of the robot is constructed from ABS plastic, each of which is instrumented with four force sensing resistors (Interlink, 402 FSR), specifically, two FSR's on each toe and heel. These sensors are located between the body of the foot and a thin foot-plate made from spring steel, Fig.6. Whenever the toe and/or the heel touches the ground, the circular rubber touch-pad (located on the foot-plate) touches the foot sensors. The corresponding signal is relayed to generate an on/off switch type output. This output serves to identify the contact configuration between the foot and the environment. Near to the toe and the heel (which are the expected contact areas) the foot-plate is supplemented with silicon rubber pads with appropriate shock absorption capability.

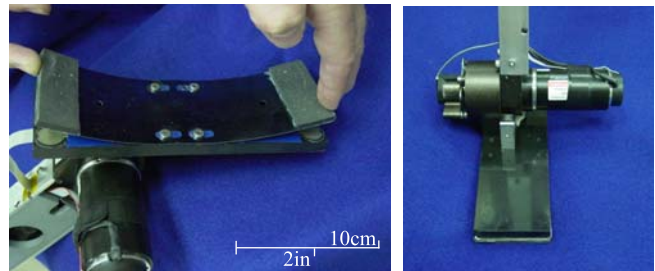


Fig. 6. The ankle joint and the foot of the robot.

#### D. Comment on Planar Walking

For the purpose of an experimental verification the robot is attached through its hip to a lever arm which keeps the biped on a circular path, with a  $1.6m$  radius while walking. This solution although not an ideal realization of a sagittal plane walk, was also utilized by [24] and [23] as a convenient platform for experimentation.

#### V. REAL-TIME CONTROL IMPLEMENTATION

The proposed closed-loop control approach is developed on a desktop PC with the real-time interface provided by MATLAB/Simulink Real Time Workshop. As follows, we describe implementation of the closed-loop control.

##### A. Feedback Information

The feedback information for the closed-loop control is provided with the contact foot sensors (FSR's), angular joint sensors (encoders) and attitude body sensor (gyroscope).

The foot sensors are used to identify the active (and inactive) constraints along the motion, imposed by foot contact with the ground. If the contact configuration is known, using the encoder measurements on the joint angles  $\varphi$  and the gyroscope on the upper body, the orientation of the body  $\theta$  can be calculated (or precisely estimated). Specifically, whenever the robot is not underactuated the absolute angular orientation for the upper body  $\theta$  is calculated using the six (encoder) measurements  $\varphi$ . Otherwise, the integrated gyroscope signal is used to provide an estimate of the absolute orientation of the upper body. Note that underactuated configurations in which case the gyroscope signal is required are expected to be short, which mitigates drift and phase lag issues with the gyroscope. Once  $\theta$  is computed, the absolute angular orientation for all the links can be obtained and the control torque computation can be started.

##### B. Computing the Actuator Torques, $\mathbf{u}$

The real-time implementation of (5) is developed utilizing standard Matlab code with Simulink/Embedded Matlab Functions. Using the model parameters  $\mathbf{E}$ ,  $\mathbf{A}$  and  $\mathbf{M}$ ,  $\mathbf{u}$  are calculated from (5) in real-time based on two standard linear algebra routines: the Cholesky factorization, and the pseudoinversion, [30], [31]. Although pseudoinversion is a relatively expensive operation, the complete control approach is shown to be real-time capable with  $1000Hz$  sampling rate on an Intel Core 2 Quad 2.4Ghz, desktop computer.

#### VI. DYNAMIC WALKING EXPERIMENT

The control approach described is applied to the robot. The experimental data from the conducted walking experiment is depicted on Fig.7. An extracted frame sequence which represents two subsequent steps is depicted on Fig.8. The walking is characterized with: average step length of  $L_{step} \approx 0.5m$ , average stepping frequency of  $f_{step} \approx 1Hz$ , average forward speed of  $v_{avg} \approx 0.5m/s$  (Froude number  $Fr = v_{avg}/\sqrt{gL_{leg}} \approx 0.2$ ), specific mechanical cost of transport  $c_{mt} \approx 0.32$ . Comparatively, this efficiency is (approximately) six times higher than human efficiency (also reproduced by

the Cornell dynamic walker), while it is five times lower than the value *estimated* for the Asimo robot, [16]. During the walking experiment, the biped utilized a characteristic ankle push-off, preferred by humans. The experiment also verified proper coordination of the robot through short ( $0.1s$ ) underactuated motion phases (when only the forward heel was on the ground).

#### VII. CONCLUSION

The authors have proposed an approach for the control of biped walking that enables dynamic walking in a fully actuated biped robot. Rather than prescribe kinematic trajectories, state dependent control torques are utilized that "encourage" patterned movement through the natural dynamics of the biped. Validation of the control method is performed on a seven link biped robot developed at the Vanderbilt University - Center for Intelligent Mechatronics. Experimental results are provided to demonstrate dynamic walking generated with the proposed control methodology.

#### REFERENCES

- [1] Y. Hurmuzlu, F. Génot, and B. Brogliato, "Modeling, stability and control of biped robots - a general framework," *Automatica*, vol. 40, no. 10, pp. 1647–1664, 2004.
- [2] M. Vukobratović and J. Stepanenko, "On the stability of antropometric systems," *Mathematical Bioscience*, vol. 15, no. 1, pp. 1–37, 1972.
- [3] M. Vukobratović, B. Borovac, D. Šurla, and D. Stokić, *Biped Locomotion*. Springer Verlag, 1990.
- [4] M. Vukobratović and B. Borovac, "Zero-moment point: Thirty five years of its life," *International Journal of Humanoid Robotics*, vol. 1, no. 1, pp. 157–173, 2004.
- [5] C.-L. Shih, "The dynamics and control of a biped walking robot with seven degrees of freedom," *Journal of Dynamic Systems, Measurement, and Control*, vol. 118, no. 4, pp. 683–690, 1996.
- [6] K. Hirai, M. Hirose, Y. Haikawa, and T. Takenaka, "The development of honda humanoid robot," *Proceedings of the 1998 IEEE ICRA*, pp. 1321–1326, 1998.
- [7] A. Goswami, "Postural stability of biped robots and the foot-rotation indicator (fri) point," *The International Journal of Robotics Research*, vol. 18, pp. 523–533, 1999.
- [8] Q. Huang, K. Yokoi, S. Kajita, K. Kaneko, H. Arai, N. Koyachi, and K. Tanie, "Planning walking patterns for a biped robot," *IEEE Transactions on Robotics and Automation*, vol. 17, no. 3, pp. 208–289, 2001.
- [9] S. Kagami, T. Kitagawa, K. Nishiwaki, T. Sugihara, M. Inaba, and H. Inoue, "A fast dynamically equilibrated walking trajectory generation method of humanoid robot," *Autonomous Robots*, vol. 12, pp. 71–82, 2002.
- [10] C. Chevallereau, D. Djoudi, and J. W. Grizzle, "Stable bipedal walking with foot rotation through direct regulation of the zero moment point," *IEEE Transactions on Robotics*, vol. 24, no. 2, pp. 390–401, 2008.
- [11] A. Takanishi, M. Ishida, Y. Yamazaki, and I. Kato, "The realization of dynamic walking by the biped walking robot WL-10RD," *Proc. Intl. Conference on Advanced Robotics*, pp. 459–466, 1985.
- [12] S. Mochon and T. A. McMahon, "Ballistic walking: An improved model," *Mathematical Biosciences*, vol. 52, pp. 241–260, 1980.
- [13] A. D. Kuo, "Choosing your steps carefully," *IEEE Robotics and Automation Magazine*, vol. 14, no. 2, pp. 18–29, 2007.
- [14] T. McGeer, "Passive dynamic walking," *The International Journal of Robotics Research*, vol. 9, no. 2, pp. 62–82, 1990.
- [15] M. J. Coleman and A. Ruina, "An uncontrolled walking toy that cannot stand still," *Physical Review Letters*, vol. 80, no. 16, pp. 3658–3661, 1998.
- [16] S. Collins, A. Ruina, R. Tedrake, and M. Wisse, "Efficient bipedal robots based on passive dynamic walkers," *Science Magazine*, vol. 307, pp. 1082–1085, 2005.

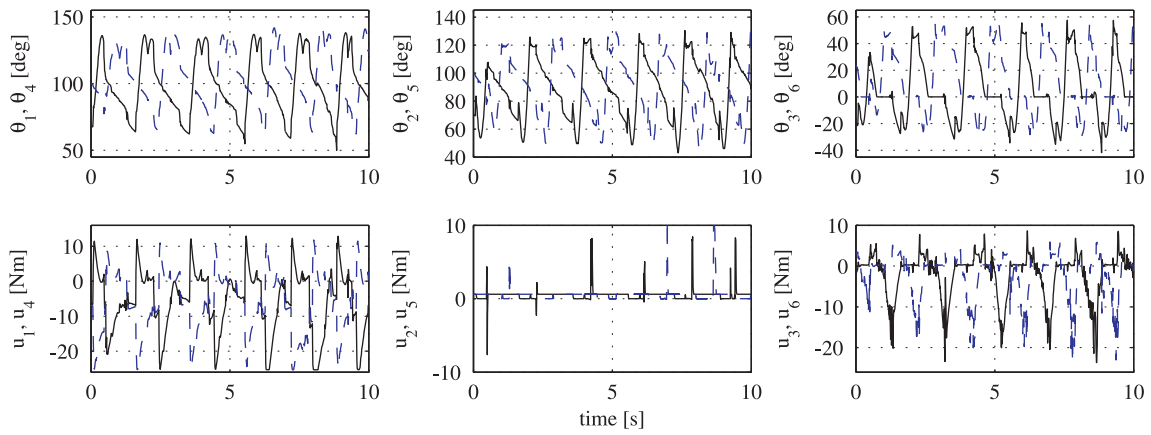


Fig. 7. Experimental data. Top: Orientation of the right leg,  $\theta_1, \theta_2, \theta_3$ , depicted with solid (black) line while the orientation of the left leg,  $\theta_4, \theta_5, \theta_6$ , is depicted with dashed (blue) line. Bottom: Control torques applied at the hip, knee and ankle joints on the right leg  $u_1, u_2, u_3$  depicted with solid (black) line, and the corresponding torques on the left leg,  $u_4, u_5, u_6$ , depicted with dashed (blue) line.

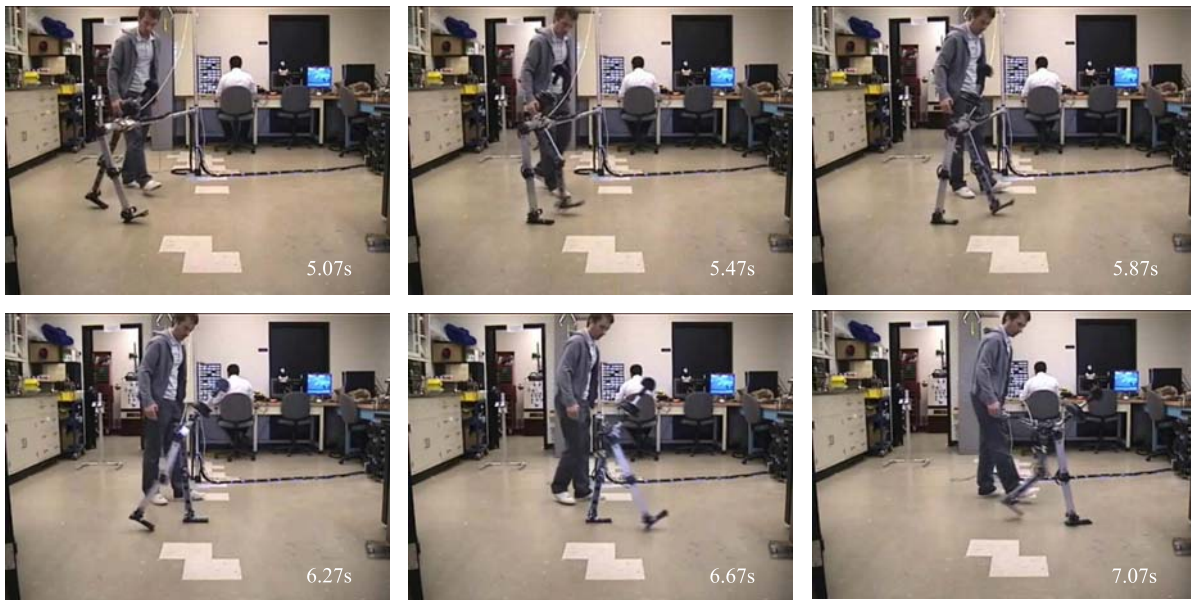


Fig. 8. Stroboscopic view of two subsequent walking steps extracted from the walking experiment.

- [17] M. Wisse, G. Felixsdal, J. van Frankenhuyzen, and B. Moyer, "Passive-based walking robot: Denis a simple efficient and lightweight biped," *IEEE Robotics and Automation Magazine*, vol. 14, no. 2, pp. 52–62, 2007.
- [18] D. G. E. Hobbelen and M. Wisse, "Controlling the walking speed in limit cycle walking," *International Journal of Robotics Research*, vol. 27, pp. 989–1005, 2008.
- [19] S. Kajita, T. Yamaura, and A. Kobayashi, "Dynamic walking control of a biped robot along a potential energy conserving orbit," *IEEE Transactions on Robotics and Automation*, vol. 8, no. 4, pp. 431–438, 1992.
- [20] O. Khatib, L. Sentis, J. Park, and J. Warren, "A whole-body dynamic behavior and control of human-like robots," *International Journal of Humanoid Robotics*, vol. 1, no. 1, p. 2943, 2004.
- [21] E. R. Westervelt, J. W. Grizzle, and D. E. Koditschek, "Hybrid zero dynamics of planar biped walkers," *IEEE Transactions on Automatic Control*, vol. 48, no. 1, pp. 42–56, 2003.
- [22] C. C. de Wit, "On the concept of virtual constraints as a tool for walking robot control and balancing," *Annual Reviews in Control*, vol. 28, pp. 157–166, 2004.
- [23] C. Chevallereau, G. Abba, Y. Aoustin, F. Plestan, E. Westervelt, C. de Wit, and J. Grizzle, "RABBIT: A testbed for advanced control theory," *IEEE Control Systems Magazine*, vol. 23, no. 5, pp. 57–78, 2003.
- [24] J. Pratt, C. M. Chew, A. Torres, P. Dilworth, and G. Pratt, "Virtual model control: An intuitive approach for bipedal locomotion," *The International Journal of Robotics Research*, vol. 20, pp. 129–143, 2001.
- [25] W. Blajer and W. Schiehlen, "Walking without impacts as a motion/force control problem," *Journal of Dynamic Systems, Measurement, and Control*, vol. 114, pp. 660–665, 1992.
- [26] D. J. Braun and M. Goldfarb, "A controller for dynamic walking in bipedal robots," *IROS, Saint Luis*, 2009 - accepted.
- [27] D. J. Braun and M. Goldfarb, "A control approach for actuated dynamic walking in biped robots," *IEEE Transactions on Robotics*, 2009 - accepted.
- [28] V. T. Inman, H. J. Ralston, and F. Todd, *Human Walking*. Baltimore, Williams and Wilkins, 1981.
- [29] D. A. Winter, *Biomechanics and Motor Control of Human Movement*. Wiley-Interscience, New York, 2 ed., 1990.
- [30] G. Golub and C. V. Loan, *Matrix Computations*. The John Hopkins University Press, 3 ed., 1996.
- [31] A. Ben-Israel and T. N. E. Greville, *Generalized Inverse: Theory and Applications*. Springer, 2003.